Journal of Hazardous Materials 162 (2009) 763–770

Contents lists available at ScienceDirect

Journal of Hazardous Materials

journal homepage: www.elsevier.com/locate/jhazmat

Band structure and visible light photocatalytic activity of multi-type nitrogen doped TiO_2 nanoparticles prepared by thermal decomposition

Fan Dong, Weirong Zhao, Zhongbiao Wu*, Sen Guo

Department of Environmental Engineering, Zhejiang University, Hangzhou 310027, China

ARTICLE INFO

Article history:
Received 15 January 2008
Accepted 21 May 2008
Available online 27 May 2008

Keywords:
Multi-type nitrogen
Band structure
Visible light
Photocatalyst
Toluene

ABSTRACT

Multi-type nitrogen doped TiO_2 nanoparticles were prepared by thermal decomposition of the mixture of titanium hydroxide and urea at 400 °C for 2 h. The as-prepared photocatalysts were characterized by X-ray diffraction (XRD), high-resolution transmission electron microscopy (HRTEM), X-ray photoelectron spectroscopy (XPS), UV–vis diffuse reflectance spectra (UV–vis DRS), and photoluminescence (PL). The results showed that the as-prepared samples exhibited strong visible light absorption due to multi-type nitrogen doped in the form of substitutional (N–Ti–O and Ti–O–N) and interstitial (π^* character NO) states, which were 0.14 and 0.73 eV above the top of the valence band, respectively. A physical model of band structure was established to clarify the visible light photocatalytic process over the as-prepared samples. The photocatalytic activity was evaluated for the photodegradation of gaseous toluene under visible light irradiation. The activity of the sample prepared from wet titanium hydroxide and urea (TiO_2–Nw, apparent reaction rate constant $k = 0.045\ min^{-1}$) was much higher than other samples including P25 ($k = 0.0013\ min^{-1}$). The high activity can be attributed to the results of the synergetic effects of strong visible light absorption, good crystallization, large surface hydroxyl groups, and enhanced separation of photoinduced carriers.

1. Introduction

Many advances have been made in TiO_2-based visible light photocatalyst in order to utilize the visible light from solar energy or artificial sources for photoinduced water splitting [1], degradation of organic pollutants in water [2,3] and air [4,5] or disinfection [6]. Asahi et al. [1] reported N-doped TiO_2 films for the first time by sputtering TiO_2 target in the mixture of N_2/Ar gas. The as-prepared catalyst showed higher photocatalytic reactivity under visible light irradiation compared to conventional TiO_2 thin films. Since then, many efforts have been made to modify TiO_2 with nonmetals, such as B [2], C [3], N [4], F [5], and S [6], to effectively extend the photoresponse of TiO_2 from the UV to the visible light region. Among these nonmetal dopants, doping TiO_2 with nitrogen has been considered one of the most effective approaches to improve photocatalytic activity of TiO_2 in visible region and provides effective routes for degradation of various environmental pollutants. In general, the N-doped TiO_2 has been successfully prepared either by reduction using gaseous NH_3 [7], oxidation of TiN [8], treating of TiO_2 and urea mixtures [9], sputtering of the TiO_2 target in N_2 atmosphere [1], or hydrolysis or hydrothermal treatment of a titanium containing precursor with NH_3 solution [10,11].

The improvement of visible light photocatalytic activity of nitrogen doped TiO_2 was usually attributed to the decrease of the band gap through hybridization of the N 2p states with O 2p states on the top of the valence band [1] or the creation of a N-induced midgap level just above the O 2p valence band maximum (VBM) [12]. However, recent electronic structure calculation indicated that there was virtually no shift of the upper edge of the O 2p valence band for the nitrogen doped TiO_2 [13]. Instead, occupied N 2p localized states appeared slightly above the valence band edge [13].

The current interesting topic of N-doped TiO_2 is to clarify the N states in TiO_2 which are usually investigated by X-ray photoelectron spectroscopy (XPS). However, the assignment of N 1s peaks is still in controversy in the literature [1,7–15]. In general, the peak of N 1s in the XPS spectra mostly lies in the range of 396–404 eV [1,7–15]. Most of reports agreed on that N 1s peak at 396–398 eV was characteristic peak of Ti–N linkages, indicating nitrogen atom is doped into the TiO_2 lattice and responsible for enhanced activity [7–10]. However, N 1s peak around 396 eV was not always observed. Nitrogen peak around 404 eV was observed by Sakthivel and Kisch [14], while the signal at 396 eV was absent. Diwald et al. [13] investigated the rutile TiO_2 crystal treated by an exposure of NH_3 gas at high temperature. The XPS analysis of N 1s peak revealed 396.5 and 399.6 eV which were comparable

* Corresponding author. Tel.: +86 571 8795 3088; fax: +86 571 8795 3088.
E-mail address: zbwu@zju.edu.cn (Z. Wu).

0304-3894/$ – see front matter © 2008 Elsevier B.V. All rights reserved.
doi:10.1016/j.jhazmat.2008.05.099

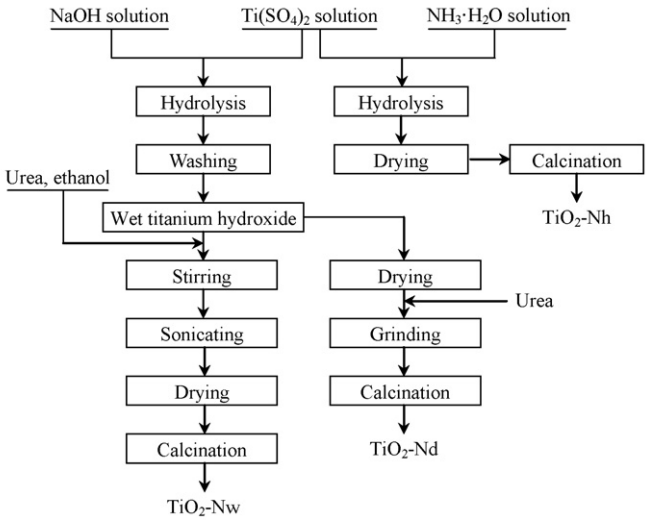

Fig. 1. The preparation procedure of photocatalyst.

to those presented by Asahi et al. [1]. However, the latter peak was suggested to be attributed to an N:H complex interstitially bound in the TiO_2 lattice. Chen and Burda [15] reported that the N 1s feature appears at 401.3 eV and was interpreted to be due to N–Ti–O linkage which was responsible for the visible light sensitization. Cong et al. [11] prepared N-doped TiO_2 nanocatalysts by a microemulsion-hydrothermal method. They found two N 1s peaks, one at 399.2 eV and another at 401.2 eV, which were present in the chemical environment of O–Ti–N and Ti–O–N. These previous works suggest that an interpretation of these N 1s states on effective visible light photocatalysis has not been clearly proposed yet.

Here, multi-type nitrogen doped TiO_2 nanoparticles with high visible light activity were prepared by thermal decomposition of the mixture of titanium hydroxide and urea for the first time. And the effect of different types of nitrogen on the band structure of TiO_2 and photocatalytic activity under visible light irradiation were investigated based on various characterization techniques and previous theoretical studies.

2. Experimental

2.1. Materials and reagents

Materials used in the experiment were titanium sulfate $Ti(SO_4)_2$ (CP, Sinopharm Chemical Reagent Co., Ltd., China), sodium hydroxide NaOH (AR, Hanghou Reagent Factory, China), Urea $CO(NH_2)_2$ (AR, Ningbo Reagent Factory, China), Ammonia solution $NH_3{\cdot}H_2O$ (AR, Hangzhou Changzheng Reagent Factory, China), ethanol C_2H_5OH (AR, Hangzhou Changzheng Reagent Factory, China), commercial TiO_2 (Degussa P25, Degussa Chemical, Germany). All reagents were used without further purification. Water was distilled and deionized before use.

2.2. Photocatalyst preparation

Multi-type N-doped TiO_2 nanoparticles were prepared by thermal decomposition method as illustrated in Fig. 1.

First, wet titanium hydroxide gel was obtained by hydrolysis of 1.0 mol/L $Ti(SO_4)_2$ with 1.0 mol/L NaOH. The obtained gel was washed with water until the concentration of the SO_4^{2-} in the rinsing water below 0.5 mg/L and then filtered. The obtained wet titanium hydroxide and 10.0 g urea were added to the 30 mL aqueous ethanol solution. The mixture was kept in dark with stirring for 1 day, sonicated and dried completely to obtain white powder. Multi-type N-doped TiO_2 nanoparticles were obtained by calcining the above white mixtures at 400 °C in air for 2 h and was labeled as TiO_2–Nw.

For comparison, the wet titanium hydroxide was dried at 80 °C for 12 h, then, the same amount of titanium hydroxide and urea was mixed by grinding and subsequently calcined at 400 °C in air for 2 h. The sample obtained was labeled as TiO_2–Nd.

N-doped TiO_2 was also prepared by hydrolysis of aqueous $Ti(SO_4)_2$ solution (20 wt.%) with 28% NH_3 solution followed by calcination [16], and labeled as TiO_2–Nh.

2.3. Characterization techniques

The crystal phases of the samples were analyzed by X-ray diffraction with Cu Kα radiation (XRD: model D/max RA, Rigaku Co., Japan). The accelerating voltage and the applied current were 40 kV and 150 mA, respectively. XPS with Al Kα X-rays ($h\nu$ = 1486.6 eV) radiation operated at 150 W (XPS: Thermo ESCALAB 250, USA) was used to investigate the surface properties and to probe the total density of the state (DOS) distribution in the valence band of the samples. The shift of the binding energy due to relative surface charging was corrected using the C 1s level at 284.8 eV as an internal standard. The morphology, structure and grain size of the samples were examined by transmission electron microscopy (TEM: JEM-2010, Japan). The UV–vis absorbance spectra were obtained for the dry-pressed disk samples using a Scan UV–vis spectrophotometer (UV–vis DRS: TU-1901, China) equipped with an integrating sphere assembly, using $BaSO_4$ as reflectance sample. The spectra were recorded at room temperature in air ranged from 230 to 800 nm. The photoluminescence (PL) spectra were measured at room temperature with a fluorospectrophotometer (PL: Fluorolog-3-Tau, France) using a Xe lamp as excitation source.

2.4. Evaluation of photocatalytic activity

Photocaytalytic degradation of toluene is chosen as the probe reaction to evaluate the activity of the prepared samples, as toluene is a typical indoor pollutant [17,18]. The photocatalytic activity experiments of the as-prepared catalysts for the oxidation of toluene in gas phase were performed at room temperature using a 1.8-L photocatalytic reactor. The catalyst was prepared by coating an ethanol suspension of the as-prepared catalyst onto a dish with diameter of 12.5 cm. The weight of catalyst used for each test was kept at 0.20 g. The dish containing catalyst was dried at 60 °C for 1 h to evaporate the ethanol and then cooled to room temperature before being used. After the catalyst-coated dish was placed in the reactor, a small amount of toluene was injected into the reactor with a micro-syringe. The analysis of toluene concentration in the reactor was conducted with a GC-FID (FULI 9790, China). The toluene vapor was allowed to reach adsorption equilibrium with the catalyst in the reactor prior to irradiation. The initial concentration of toluene after adsorption equilibrium was controlled at 150 mg/m^3. A 150-W Xe lamp was placed above the reactor as the light source. For visible light photocatalysis, a glass optical filter was inserted to cut off the short wavelength components (λ < 425 nm). The initial temperature was 25 ± 1 °C by cooling air. The initial relative humidity was controlled by a $CaCl_2$ dryer connected to the photoreactor.

The photocatalytic activity of the catalyst samples can be quantitatively evaluated by comparing the apparent reaction rate constants. The photocatalytic oxidation of toluene is a pseudo-

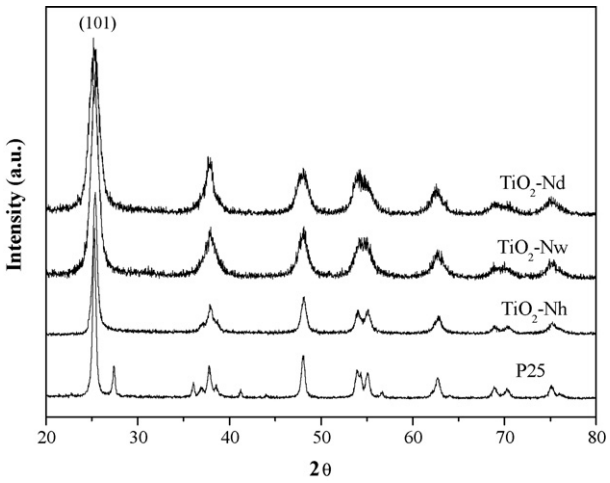

Fig. 2. X-ray diffraction patterns of TiO_2–Nd, TiO_2–Nw, TiO_2–Nh samples and P25.

first-order reaction and its kinetics may be expressed as follows: $\ln(C_0/C) = kt$ [19,20], where k is the apparent reaction rate constant, C_0 and C are the initial concentration and the reaction concentration of toluene, respectively.

3. Results and discussion

3.1. Structure and morphology

The XRD patterns of the as-prepared N-doped TiO_2 samples and P25 are shown in Fig. 2. It can be seen from Fig. 2 that the pattern of as-prepared samples can be indexed to TiO_2 in the anatase phase only (JCPDS 21-1272). The strongest peak at $2\theta = 25.3^\circ$ is representative for (1 0 1) anatase phase reflections. From the full width at half-maximum of the diffraction pattern, the crystal sizes can be calculated by using Scherrer's equation [21]. The as-calculated crystal sizes of sample TiO_2–Nw, TiO_2–Nd and TiO_2–Nh were 9.2, 8.1 and 13.7 nm, respectively. The difference in crystal size may be ascribed to the different preparation conditions which affect the crystal development. P25 is made of 20% rutile and 80% anatase, which usually exhibits high photocatalytic activity because of its phase composition [19,20].

The structure of N-doped TiO_2 powders are further investigated by TEM and high-resolution transmission electron microscopy (HRTEM) image as shown in Fig. 3. The images (Figs. 3a and c) reveal that TiO_2–Nw and TiO_2–Nd samples consist of agglomerates of primary particles with average diameters of 8–10 nm, which are in agreement with the crystallite sizes calculated from the XRD patterns. The corresponding HRTEM image of sample TiO_2–Nw (Fig. 3b) shows clear lattice fringes, which allows for identification

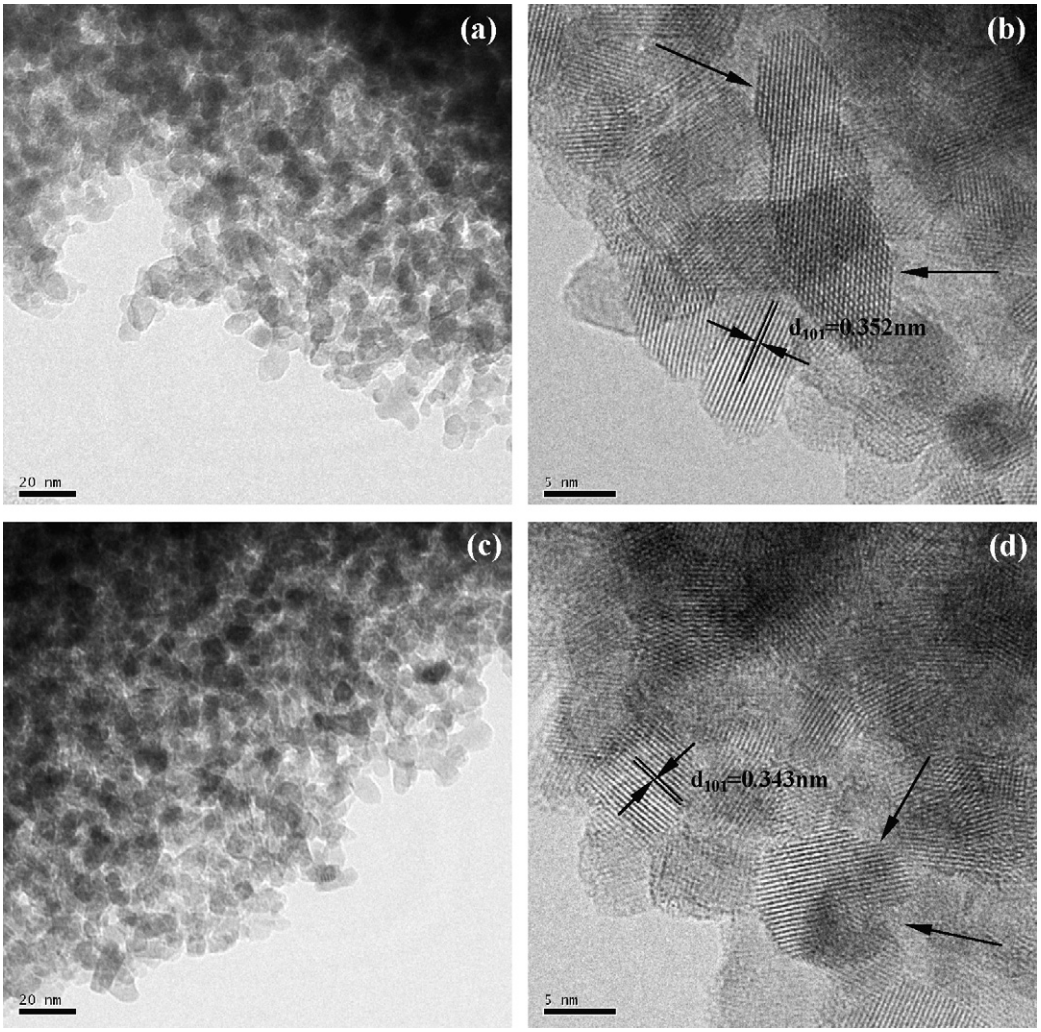

Fig. 3. TEM and HRTEM images of TiO_2–Nw (a and b) and TiO_2–Nd (c and d) samples.

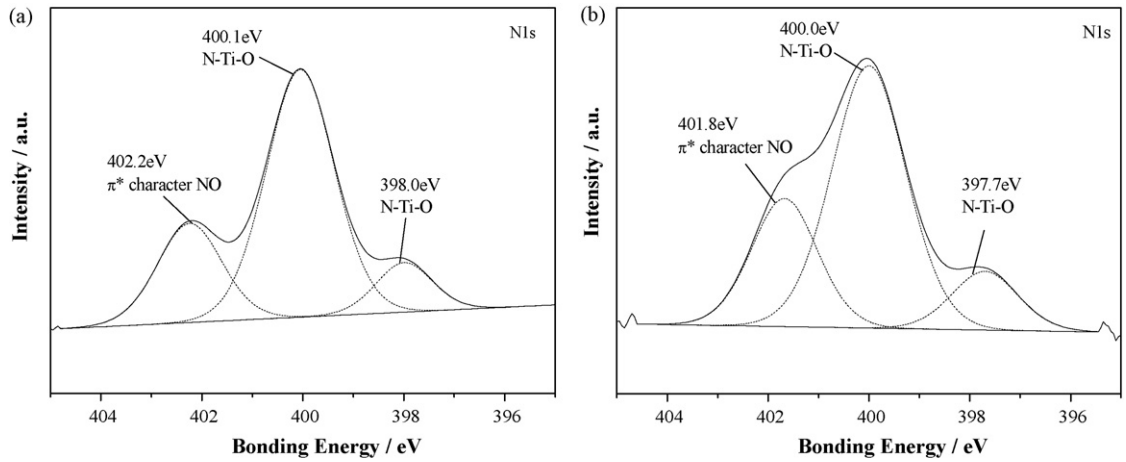

Fig. 4. High-resolution XPS spectra of N 1s region of the TiO_2–Nw (a) and TiO_2–Nd (b).

of crystallographic spacing and indicates that the prepared TiO_2–Nw nanoparticles are well crystalline. The lattice fringes of 0.352 nm matches that of the (1 0 1) crystallographic plane of anatase TiO_2 [22]. Some crystals with clear edges can also be seen from Fig. 3b. As to the sample TiO_2–Nd (Fig. 3d), the lattice fringes of (1 0 1) crystallographic plane is calculated to be 0.343 nm which is smaller than the standard value of 0.352 nm. This result demonstrated that the crystallinity of sample TiO_2–Nw was better than that of TiO_2–Nd, which was consistent with the above XRD result. The difference in crystallinity of the two samples lied in different preparation conditions. Homogeneous mixing of wet titanium hydroxide and urea may promote the development of anatase TiO_2 crystal.

3.2. XPS analysis

The chemical state of the doped nitrogen in the TiO_2 is investigated by core level X-ray photoelectron spectroscopy (CL XPS) and shown in Fig. 4. Fig. 4a shows the high-resolution XPS spectra of the N 1s region, taken on the surface of TiO_2–Nw powders. The N 1s region can be fitted into three peaks, located at 398.0, 400.1 and 402.2 eV, respectively. These peaks are the result of the diffusion of the nitrogen atoms during the thermal treatment and indicate three different types of N states. Recently, theoretical studies about N-doped TiO_2 have been performed by Di Valentin et al. [23] to clarify the origin of visible light activity. It was found that nitrogen impurities in TiO_2 band structure were expected to result from substitutional and interstitial nitrogen atoms and higher core level binding energy accounted for the interstitial configuration as proved by DFT calculations [13]. According to the N 1s peaks, the observed peak at 398.0 eV is due to the presence of substitutional nitrogen in the N–Ti–O structure [24,25]. Based on the reports of Saha and Tompkins [26] and Gyorgy et al. [27], the binding energy of substitutional N in oxidized nitrogen state such as Ti–N–O linkages should appear above 400 eV. The observed peak at higher value of 402.2 eV accounts for the presence of interstitial N state as π* character NO in the N-doped TiO_2 sample [23]. From the above observations it can be concluded that the chemical states of the nitrogen doped into TiO_2 may be various and coexist in the form of substitutional N–Ti–O and Ti–O–N (N_s), as well as interstitial π* character NO (N_i). These multi-type doping may promote the stabilization which was interpreted as interspecies redox processes [28]. The multi-type nitrogen doping may induce the complex electronic states in the band gap, which will be discussed later.

Table 1
Results of curve-fitting of high-resolution XPS spectra for the O 1s region and photocatalytic activities of TiO_2–Nw and TiO_2–Nw samples

Sample		O_L (Ti–O)	O_H (–OH)	$k \times 10^2$ (min^{-1})
TiO_2–Nw	E_b	529.9	531.5	4.5
	r_i (%)	74.7	25.3	
TiO_2–Nh	E_b	530.2	531.7	1.5
	r_i (%)	80.0	20.0	

Note: r_i indicates the atomic ratio of each contribution to the total of all the two kinds of oxygen contributions.

The nitrogen content of TiO_2–Nw sample is also estimated by CL XPS to be about 2.18%. Similar results can be obtained for the sample TiO_2–Nd (Fig. 4b) from CL XPS except that the nitrogen content is higher (4.20%) than that of TiO_2–Nw.

Fig. 5 shows the CL XPS of O 1s region of TiO_2–Nw and TiO_2–Nw samples. It can be seen from Fig. 5 and Table 1 that the binding energy of O_L and O_H are 529.9 (530.2) and 531.5 (531.7) eV for the sample TiO_2–Nw and TiO_2–Nd, respectively. The O_L XPS is mainly attributed to the contribution of Ti–O in TiO_2 crystal lattice, and the O_H XPS is closely related to the hydroxyl groups (–OH) resulting mainly from the chemisorbed water [19,29]. It can also be seen from Table 1 that the content of surface hydroxyl groups (r_i, %) is much higher in the TiO_2–Nw than that of TiO_2–Nd sample. The increase

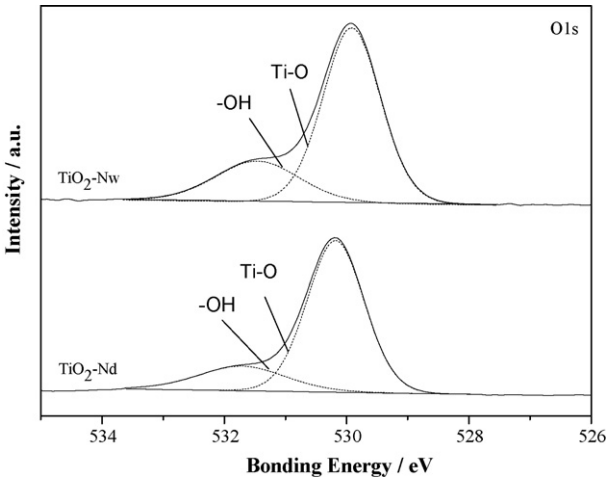

Fig. 5. High-resolution XPS spectra of the O 1s region of TiO_2–Nw and TiO_2–Nw samples.

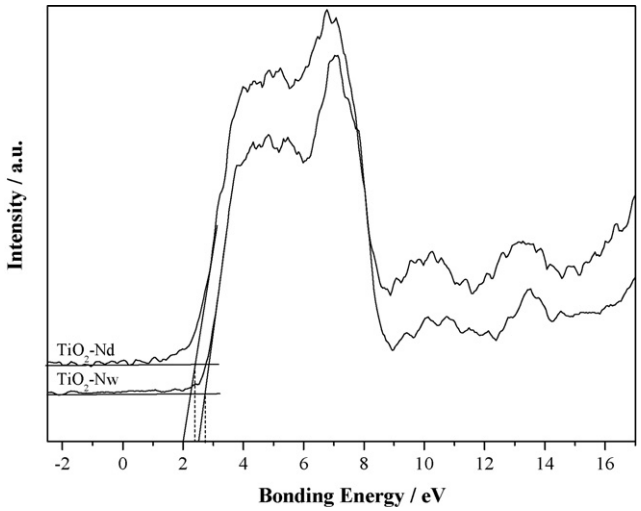

Fig. 6. VB XPS spectra of TiO_2–Nd and TiO_2–Nw samples.

in content of surface hydroxyl groups was advantageous for trapping more photogenerated holes and thus preventing electron–hole recombination [29]. This result indicated that wet titanium hydroxide precursor can increase the surface hydroxyl group density of the resultant catalyst.

According to the CL XPS results, N states exist in both substitutional and interstitial N states. The electronic structure of N-doped TiO_2 is further investigated by valence band X-ray photoelectron spectroscopy (VB XPS). Fig. 6 presents the VB XPS spectra of TiO_2–Nd and TiO_2–Nw samples. In Fig. 6, the valence O 2p-derived VBM of TiO_2–Nw and TiO_2–Nd are determined to be 2.7 and 2.4 eV below Fermi level by conventional linear extrapolation method, which are smaller than the value (3.2 eV) of undoped TiO_2 [30]. Combined with CL XPS results, it can be deduced that the substitutional and interstitial N states lie higher above the O 2p valence band edge. This deduction is also confirmed by recent theoretical studies [23,31].

3.3. Optical properties

Usually, N doping obviously affects light absorption characteristics of TiO_2. Fig. 7 shows the UV–vis diffuse reflectance spectra (UV–vis DRS) of the as-prepared samples and P25. The P25 powder shows an onset of absorption at 405 nm as commonly observed, while doping of N greatly enhances the absorption of TiO_2–Nd and TiO_2–Nw samples in the UV–vis spectrum and effectively extends the absorption edge into the visible light region. N doping contributed to the localized N 2p states in the band structure in the form of substitutional and interstitial N states, which are responsible for visible light absorption [23,32]. These results are consistent with VB XPS spectra. It is interesting to note that the absorption in UV region of the sample TiO_2–Nw is similar to that of pure TiO_2. One possible explanation is that the sample TiO_2–Nw contains two kinds of TiO_2, doped and undoped TiO_2 [4]. It is acceptable because the content of nitrogen in the as-prepared sample is relatively low compared to lattice oxygen.

PL emission spectra have been widely used to investigate the efficiency of charge carrier trapping, migration, and transfer in order to understand the fate of electron–hole pairs in semiconductor particles since PL emission results from the recombination of free carriers [11,33–35].

Fig. 8 shows the PL spectra (300 nm excitation source) of TiO_2–Nd and TiO_2–Nw samples. It can be seen from Fig. 8 that there are four peaks located at 387 (peak I), 437 (peak II), 470 (peak III) and 558 nm (peak IV). Peak I is ascribed to the emission of the intrinsic band gap transition, peak II is due to substitutional N states, peak III originates from the charge transfer transition of an oxygen vacancy trapped electron, and peak IV comes from the interstitial N states [11,33]. Generally speaking, the lower PL intensity of the doped sample indicates a lower recombination rate. The PL intensity of TiO_2–Nw is lower than that of TiO_2–Nd, indicating that the charge separation rate of TiO_2–Nw is higher than that of TiO_2–Nd. Higher concentration of nitrogen doped in TiO_2 may become the recombination site [7], thus the PL intensity of sample TiO_2–Nd with higher N content increased.

3.4. Presumed band structure and visible light photocatalytic activities

Nitrogen doping can form new states just above the valence band for the substitutional or interstitial nitrogen, which could make TiO_2 absorb visible light [12,13,32]. Di Valentin et al. [23] provided theoretical evidence that for substitutional N-doped anatase TiO_2, the visible light response arises from occupied N 2p localized states slightly above the valence band edge, whereas for interstitial N-doped anatase TiO_2, the visible light

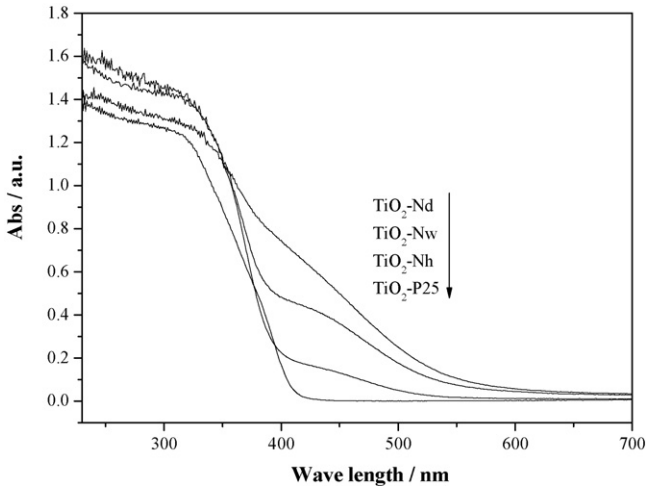

Fig. 7. UV–vis diffuse reflectance spectra of as-prepared samples and P25.

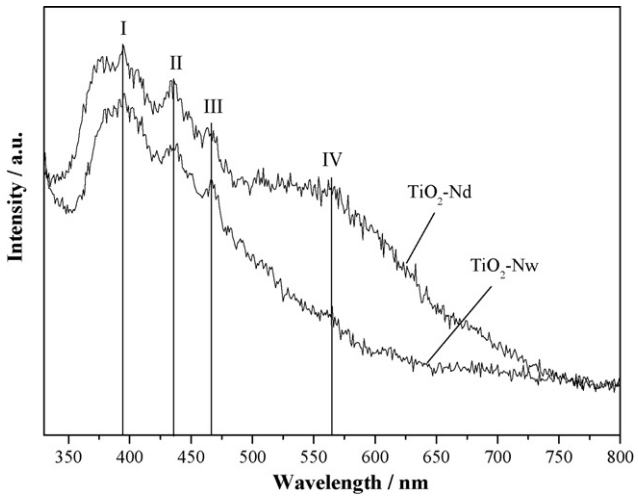

Fig. 8. Photoluminescence spectra of TiO_2–Nd and TiO_2–Nw samples (excitation source: 300 nm).

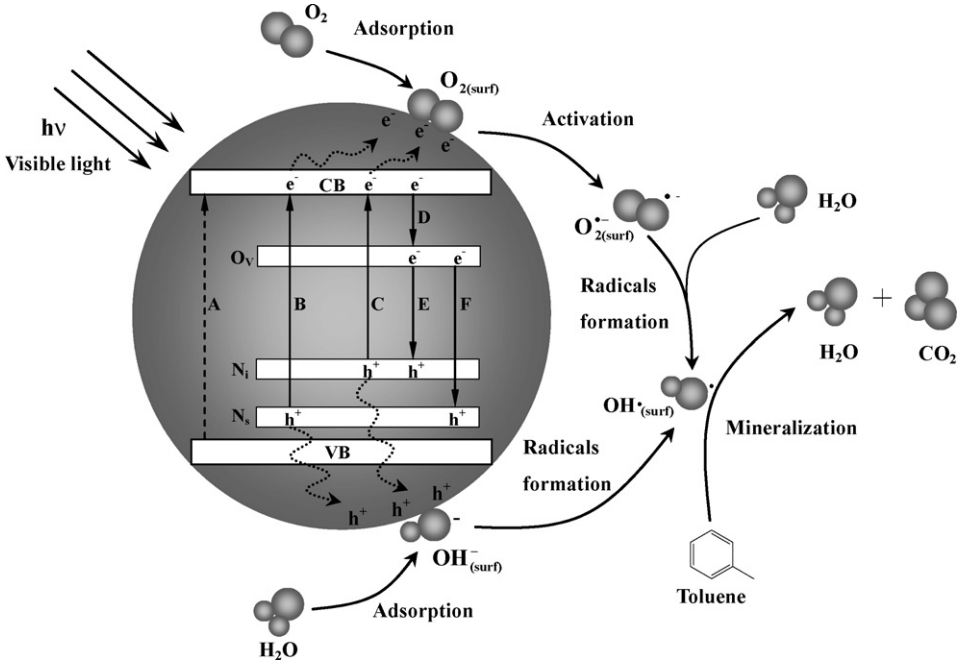

Fig. 9. Proposed band structure of multi-type nitrogen doped TiO_2 and visible light photocatalytic process.

response arises from occupied π^* character N–O localized states slightly above the valence band edge. The highest localized state for the substitutional N state is 0.14 eV above the top of the valence band and 0.73 eV for the interstitial N state. It can also be testified by the UV–vis DRS, PL and VB XPS (Figs. 6–8). DFT calculations suggested that N-doping favored the formation of O vacancy (O_V) which was experimentally found to be about 0.8 eV below the bottom of the conduction band [13,32,36]. On the basis of the above analysis, a schematic diagram of band gap structure is proposed, as illustrated in Fig. 9. The energy of the visible light is not sufficient to excite electrons from the valence band, as the TiO_2 anatase band gap is 3.2 eV, i.e., the process A cannot occur. After nitrogen doping, the electron can be excited from the N impurity levels (N_s and N_i) to the conduction band (process B and C), and then energetically favorably trapped by O vacancies (process D). The photoinduced electrons in the O_V state and conduction band may recombine with the holes in the N impurity levels (process E and F) to give rise to PL signals. The substitutional nitrogen state (N_s) and interstitial nitrogen state (N_i) are directly responsible for the origin of visible light induced photocatalysis. As the mechanism of nonmetal doping is somewhat similar, this model may be helpful to understand the mechanism of visible light photocatalysis over other nonmetal (such as B or C) doped TiO_2 photocatalyst.

The process of visible light photocatalytic oxidation of toluene is described in Fig. 9. First, holes in the impurity level (including N_s and N_i states) and electrons in conduction band were generated (Eqs. (1) and (2)) under visible light irradiation.

$$TiO_2 - N_s + vis \rightarrow h^+ + e_{CB}{}^- \quad (1)$$

$$TiO_2 - N_i + vis \rightarrow h^+ + e_{CB}{}^- \quad (2)$$

Then, the holes and electrons will react with OH^- and molecule O_2 on the catalyst surface to form •OH radicals and $O_2{}^{\bullet -}$ superoxide anion radicals [37], respectively (Eqs. (3)–(5)). The $O_2{}^{\bullet -}$ radicals then interact with H_2O adsorbed to produce more •OH radicals (Eq. (6)), which are known to be the most oxidizing species [37].

$$H_2O \Leftrightarrow OH_{(surf)}{}^- + H^+ \quad (3)$$

$$OH_{(surf)}{}^- + h^+ \rightarrow {}^{\bullet}OH \quad (4)$$

$$e_{CB}{}^- + O_2 \rightarrow O_{2(surf)}{}^{\bullet -} \quad (5)$$

$$O_{2(surf)}{}^{\bullet -} + H_2O \rightarrow {}^{\bullet}OH + OH^- \quad (6)$$

Finally, these •OH radicals react with gaseous toluene to mineralize it (Eq. (7)).

$$^{\bullet}OH + C_7H_8 \rightarrow CO_2 + H_2O \quad (7)$$

As can be seen from the above equations that the surface hydroxyl groups accept holes generated by visible light irradiation to form hydroxyl radicals thus prevent electron–hole recombination [37]. Therefore, it is expected that a greater number of hydroxyl groups yield a higher photocatalytic activity [22,29].

To evaluate the visible light photocatalytic activity of as-prepared samples, photodegradation of toluene in gas phase as a test reaction was performed. The results of the photocatalytic activities are shown in Fig. 10. It can be seen from Fig. 10 that TiO_2–Nw sample is superior to other samples. Generally speaking, the activity of photocatalyst is strongly influenced by its light absorption [10,38]. Tseng et al. [39] found that the photocatalytic activity of C-modified TiO_2 samples under visible light was proportional to their visible light absorption. However, it can be seen from Figs. 7 and 10 that the visible light activity of the as-prepared samples is not always proportional to its visible absorption. P25 shows almost no visible light activity as it cannot utilize visible light. The sample TiO_2–Nh ($k = 0.0041\ min^{-1}$) exhibits the lowest photocatalytic activity under visible light irradiation due to its weak visible light absorption and large crystal size. The photocatalyst TiO_2–Nd ($k = 0.015\ min^{-1}$) having the strongest visible light absorption does not exhibit best visible light activity. The sample TiO_2–Nw ($k = 0.045\ min^{-1}$) exhibits the best activity which can be probably ascribed to the following two factors. First, sample TiO_2–Nw contains large surface hydroxyl groups, which is beneficial to prevent electron–hole recombination, as discussed previously. Second, good crystallization of it reduces the recombination rate of the photogenerated electron–hole pairs due to the decrease in the number of the defects [40]. The enhanced separation

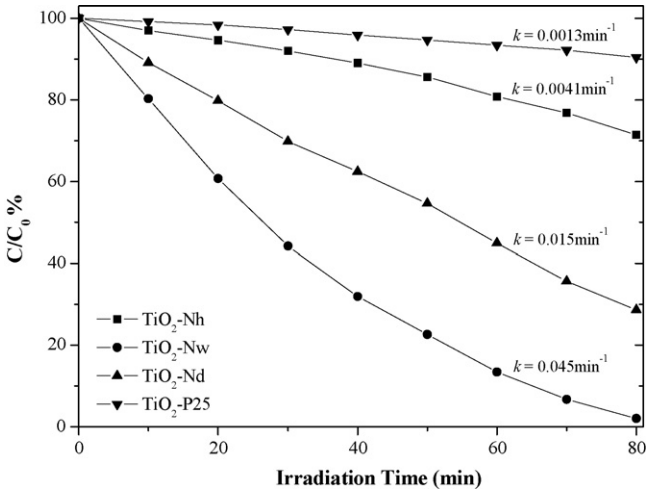

Fig. 10. Toluene photodegradation of as-prepared samples and P25 under visible light irradiation (425 nm < λ < 700 nm).

of photoinduced carriers is also evidenced by the PL result (Fig. 8).

4. Conclusions

(1) Multi-type N-doped TiO_2 was prepared by thermal decomposition of titanium hydroxide and urea mixtures. The samples showed strong visible light absorption due to the fact that the N coexisted in multi-form of substitutional N–Ti–O and Ti–O–N, as well as π^* character interstitial NO and the subsequent formation of localized nitrogen state and oxygen vacancies.

(2) A physical model of band structure was constructed to elucidate the role of different types of nitrogen in visible light photocatalysis. Substitutional N state (N_s) and interstitial N state (N_i) are 0.14 and 0.73 eV above the top of the valence band respectively, while the O vacancy (O_V) is about 0.8 eV below the bottom of the conduction band. These impurity levels were responsible for the electronic origin for the visible light absorption and photocatalytic properties of the multi-type nitrogen doped TiO_2. This model can be applied to understand visible light induced photocatalyst over other nonmetal doped TiO_2.

(3) The visible light induced photocatalytic activity of the as-prepared TiO_2–Nw sample was much higher than those of TiO_2–Nd and TiO_2–Nh samples and Degussa P25. The high activity can be ascribed to strong absorption in the visible light region, good crystallization, large surface hydroxyl group and enhanced separation of photoinduced carriers.

Acknowledgements

This research was financially supported by the Chinese Key Technology R&D Program of the Eleventh Five-year Plan (2006BAJ02A08), the Hangzhou Science & Technology Development Program (20061133B27) and the Research Fund for the Doctoral Program of Higher Education (20070335197).

References

[1] R. Asahi, T. Morikawa, T. Ohwaki, K. Aoki, Y. Taga, Visible-light photocatalysis in nitrogen-doped titanium oxides, Science 293 (2001) 269–271.
[2] W. Zhao, W.H. Ma, C.C. Chen, J.C. Zhao, Z.G. Shuai, Efficient degradation of toxic organic pollutants with $Ni_2O_3/TiO_{2-x}B_x$ under visible irradiation, J. Am. Chem. Soc. 126 (2004) 4782–4783.
[3] W.J. Ren, Z.H. Ai, F.L. Jia, L.Z. Zhang, X.X. Fan, Z.G. Zou, Low temperature preparation and visible light photocatalytic activity of mesoporous carbon-doped crystalline TiO_2, Appl. Catal. B 69 (2007) 138–144.
[4] J.G. Yu, M.H. Zhou, B. Cheng, X.J. Zhao, Preparation, characterization and photocatalytic activity of in situ N,S-codoped TiO_2 powders, J. Mol. Catal. A: Chem. 246 (2006) 176–184.
[5] D. Li, H. Haneda, N.K. Labhsetwar, S. Hishita, N. Ohashi, Visible-light-driven photocatalysis on fluorine-doped TiO_2 powders by the creation of surface oxygen vacancies, Chem. Phys. Lett. 401 (2005) 579–584.
[6] J.C. Yu, W.K. Ho, J.G. Yu, H. Yip, P.K. Wong, J.C. Zhao, Efficient visible-light-induced photocatalytic disinfection on sulfur-doped nanocrystalline titania, Environ. Sci. Technol. 39 (2005) 1175–1179.
[7] H. Irie, Y. Watanabe, K. Hashimoto, Nitrogen-concentration dependence on photocatalytic activity of $TiO_{2-x}N_x$ powders, J. Phys. Chem. B 107 (2003) 5483–5486.
[8] T. Morikawa, R. Asahi, T. Ohwaki, K. Aoki, Y. Taga, Band-gap narrowing of titanium dioxide by nitrogen doping, Jpn. J. Appl. Phys. Part 2 40 (2001) L561–L563.
[9] S. Yin, K. Ihara, M. Komatsu, Q.W. Zhang, F. Saito, T. Kyotani, T. Sato, Low temperature synthesis of $TiO_{2-x}N_y$ powders and films with visible light responsive photocatalytic activity, Solid State Commun. 137 (2006) 132–137.
[10] Y.Q. Wang, X.J. Yu, D.Z. Sun, Synthesis, characterization, and photocatalytic activity of $TiO_{2-x}N_x$ nanocatalyst, J. Hazard. Mater. 144 (2007) 328–333.
[11] Y. Cong, J.L. Zhang, F. Chen, M. Anpo, Synthesis and characterization of nitrogen-doped TiO_2 nanophotocatalyst with high visible light activity, J. Phys. Chem. C 111 (2007) 6976–6982.
[12] R. Nakamura, T. Tanaka, Y. Nakato, Mechanism for visible light responses in anodic photocurrents at N-doped TiO_2 film electrodes, J. Phys. Chem. B 108 (2004) 10617–10620.
[13] C. Di Valentin, E. Finazzi, G. Pacchioni, A. Selloni, S. Livraghi, M.C. Paganini, E. Giamello, N-doped TiO_2: theory and experiment, Chem. Phys. 339 (2007) 28–35.
[14] S. Sakthivel, H. Kisch, Photocatalytic and photoelectrochemical properties of nitrogen-doped titanium dioxide, Chem. Phys. Chem. 4 (2003) 487–490.
[15] X.B. Chen, C. Burda, Photoelectron spectroscopic investigation of nitrogen-doped titania nanoparticles, J. Phys. Chem. B 108 (2004) 15446–15449.
[16] T. Ihara, M. Miyoshi, Y. Iriyama, O. Matsumoto, S. Sugihara, Visible-light-active titanium oxide photocatalyst realized by an oxygen-deficient structure and by nitrogen doping, Appl. Catal. B 42 (2003) 403–409.
[17] R. Yang, Y.P. Zhang, Q.J. Xu, J.H. Mo, A mass transfer based method for measuring the reaction coefficients of a photocatalyst, Atmos. Environ. 41 (2007) 1221–1229.
[18] Y.P. Zhang, R. Yang, Q.J. Xu, J.H. Mo, Characteristics of photocatalytic oxidation of toluene, benzene, and their mixture, J. Air Waste Manage. Assoc. 57 (2007) 94–101.
[19] J.G. Yu, G.H. Wang, B. Cheng, M.H. Zhou, Effects of hydrothermal temperature and time on the photocatalytic activity and microstructures of bimodal mesoporous TiO_2 powders, Appl. Catal. B 69 (2007) 171–180.
[20] J.G. Yu, Y.R. Su, B. Cheng, Template-free fabrication and enhanced photocatalytic activity of hierarchical macro-/mesoporous titania, Adv. Funct. Mater. 17 (2007) 1984–1990.
[21] M.C. Yan, F. Chen, J.L. Zhang, M. Anpo, Preparation of controllable crystalline titania and study on the photocatalytic properties, J. Phys. Chem. B 109 (2005) 8673–8678.
[22] Z.B. Wu, Z.L. Gu, W.R. Zhao, H.Q. Wang, Photocatalytic oxidation of gaseous benzene over nanosized TiO_2 prepared by solvothermal method, Chin. Sci. Bull. 52 (2007) 3061–3067.
[23] C. Di Valentin, G. Pacchioni, A. Selloni, S. Livraghi, E. Giamello, Characterization of paramagnetic species in N-doped TiO_2 powders by EPR spectroscopy and DFT calculations, J. Phys. Chem. B 109 (2005) 11414–11419.
[24] M. Sathish, B. Viswanathan, R.P. Viswanath, C.S. Gopinath, Synthesis, characterization, electronic structure, and photocatalytic activity of nitrogen-doped TiO_2 nanocatalyst, Chem. Mater. 17 (2005) 6349–6353.
[25] H.X. Li, J.X. Li, Y.I. Huo, Highly active TiO_2N photocatalysts prepared by treating TiO_2 precursors in NH_3/ethanol fluid under supercritical conditions, J. Phys. Chem. B 110 (2006) 1559–1565.
[26] N.C. Saha, H.G. Tompkins, Titanium nitride oxidation chemistry: an x-ray photoelectron spectroscopy study, J. Appl. Phys. 72 (1992) 3072–3079.
[27] E. Gyorgy, A.P. del Pino, P. Serra, J.L. Morenza, Depth profiling characterisation of the surface layer obtained by pulsed Nd:YAG laser irradiation of titanium in nitrogen, Surf. Coat. Technol. 173 (2003) 265–270.
[28] C. Di Valentin, G. Pacchioni, A. Selloni, Theory of carbon doping of titanium dioxide, Chem. Mater. 17 (2005) 6656–6665.
[29] J.G. Yu, H.G. Yu, B. Cheng, M.H. Zhou, X.J. Zhao, Enhanced photocatalytic activity of TiO_2 powder (P25) by hydrothermal treatment, J. Mol. Catal. A: Chem. 253 (2006) 112–118.
[30] M. Batzill, E.H. Morales, U. Diebold, Influence of nitrogen doping on the defect formation and surface properties of TiO_2 rutile and anatase, Phys. Rev. Lett. 96 (2006) (art. no. 026103).
[31] A. Nambu, J. Graciani, J.A. Rodriguez, Q. Wu, E. Fujita, J.F. Sanz, N doping of TiO_2 (1 1 0): photoemission and density-functional studies, J. Chem. Phys. 125 (2006) (art. no. 094706).

[32] S. Livraghi, M.C. Paganini, E. Giamello, A. Selloni, C. Di Valentin, G. Pacchioni, Origin of photoactivity of nitrogen-doped titanium dioxide under visible light, J. Am. Chem. Soc. 128 (2007) 15666–15671.
[33] J.L. Zhang, Y. Hu, M. Matsuoka, H. Yamashita, M. Minagawa, H. Hidaka, M. Anpo, Relationship between the local structures of titanium oxide photocatalysts and their reactivities in the decomposition of NO, J. Phys. Chem. B 105 (2001) 8395–8398.
[34] J.C. Yu, J.G. Yu, W.K. Ho, Z.T. Jiang, L.Z. Zhang, Effects of F^- doping on the photocatalytic activity and microstructures of nanocrystalline TiO_2 powders, Chem. Mater. 14 (2002) 3808–3816.
[35] J.G. Yu, H.G. Yu, B. Cheng, X.J. Zhao, J.C. Yu, W.K. Ho, The effect of calcination temperature on the surface microstructure and photocatalytic activity of TiO_2 thin films prepared by liquid phase deposition, J. Phys. Chem. B 107 (2003) 13871–13879.
[36] M.A. Henderson, W.S. Epling, C.H.F. Peden, C.L. Perkins, Insights into photoexcited electron scavenging processes on TiO_2 obtained from studies of the reaction of O_2 with OH groups adsorbed at electronic defects on TiO_2 (1 1 0), J. Phys. Chem. B 107 (2003) 534–545.
[37] K. Nagaveni, M.S. Hegde, N. Ravishankar, G.N. Subbanna, G. Madras, Synthesis and structure of nanocrystalline TiO_2 with lower band gap showing high photocatalytic activity, Langmuir 20 (2004) 2900–2907.
[38] M.H. Zhou, J.G. Yu, B. Cheng, Effects of Fe-doping on the photocatalytic activity of mesoporous TiO_2 powders prepared by an ultrasonic method, J. Hazard. Mater. 137 (2006) 1838–1847.
[39] Y.H. Tseng, C.S. Kuo, C.H. Huang, Y.Y. Li, P.W. Chou, C.L. Cheng, M.S. Wong, Visible-light-responsive nano-TiO_2 with mixed crystal lattice and its photocatalytic activity, Nanotechnology 17 (2006) 2490–2497.
[40] J.G. Yu, L.J. Zhang, B. Cheng, Y.R. Su, Hydrothermal preparation and photocatalytic activity of hierarchically sponge-like macro-/mesoporous titania, J. Phys. Chem. C 111 (2007) 10582–10589.